

Propagation of H and He Cosmic Ray Isotopes in the Galaxy: Astrophysical and Nuclear Uncertainties

Nicola Tomassetti

Abstract

Observations of light isotopes in cosmic rays provide valuable information on their origin and propagation in the Galaxy. Using the data collected by the AMS-01 experiment in the range ~ 0.2 - 1.5 GeV nucleon $^{-1}$, we compare the measurements on ^1H , ^2H , ^3He , and ^4He with calculations for interstellar propagation and solar modulation. These data are described well by a diffusive-reacceleration model with parameters that match the B/C ratio data, indicating that He and heavier nuclei such as C-N-O experience similar propagation histories. Close comparisons are made within the astrophysical constraints provided by the B/C ratio data and within the nuclear uncertainties arising from errors in the production cross section data. The astrophysical uncertainties are expected to be dramatically reduced by the data upcoming from AMS-02, so that the nuclear uncertainties will likely represent the most serious limitation on the reliability of the model predictions. On the other hand, we find that secondary-to-secondary ratios such as $^2\text{H}/^3\text{He}$, $^6\text{Li}/^7\text{Li}$ or $^{10}\text{B}/^{11}\text{B}$ are barely sensitive to the key propagation parameters and can represent a useful diagnostic test for the consistency of the calculations.

Keywords cosmic rays — acceleration of particles — nuclear reactions, nucleosynthesis, abundances

1 Introduction

Secondary Cosmic Ray (CR) isotopes such as ^2H , ^3He and Li-Be-B are believed to be produced as a result of nuclear interactions primary CRs such as ^1H , ^4He or C-N-O with the gas nuclei of the interstellar medium (ISM). The secondary CR abundances depend on the intensity of their

progenitors nuclei, their production rate and their transport in the turbulent magnetic fields (Strong et al. 2007). Secondary to primary ratios such as $^2\text{H}/^4\text{He}$, $^3\text{He}/^4\text{He}$ or B/C be used to study the CR propagation processes in the Galaxy. The B/C ratio is widely used to determine the key parameters of propagation models. In fact the B/C ratio is measured by several experiments between ~ 100 MeV and ~ 1 TeV of kinetic energy per nucleon. The CR propagation physics is also connected with the indirect search of dark matter particles. In this context the CR propagation models, once tuned to agree with the B/C ratio, are used to compute the secondary production for other rare species such as \bar{p} or \bar{d} , that provides the *astrophysical background* for the search of new physics signals (Donato et al. 2008; Evoli et al. 2011; Salati et al. 2010). Clearly, understanding the CR propagation processes is crucial for modeling both the CR signal and the background. Furthermore, these studies assume that all the CR species experience the same propagation effects in their journey throughout the ISM (Putze et al. 2010; Trotta et al. 2011). It is therefore important to test the CR propagation with nuclei of different mass-to-charge ratios. This issue of the *universality* of CR propagation histories was also studied in Webber (1997) and, recently, in Coste et al. (2011).

In this work we use the recent AMS-01 observations for the $^2\text{H}/^4\text{He}$ and $^3\text{He}/^4\text{He}$ ratios and compare them with the expected ratios based on interstellar and heliospheric propagation calculations. The aim of this work is to determine whether the AMS-01 observations are consistent with the propagation calculations derived from heavier nuclei (mainly from B/C data). This consistency is inspected within two classes of model uncertainties: the *astrophysical uncertainties*, which are related to the knowledge of the CR transport parameters given by the B/C ratio, and the *nuclear uncertainties*, which arise from the ^2H and ^3He production cross sections.

Nicola Tomassetti

INFN - Sezione di Perugia, 06122 Perugia, Italy.

E-mail: nicola.tomassetti@pg.infn.it

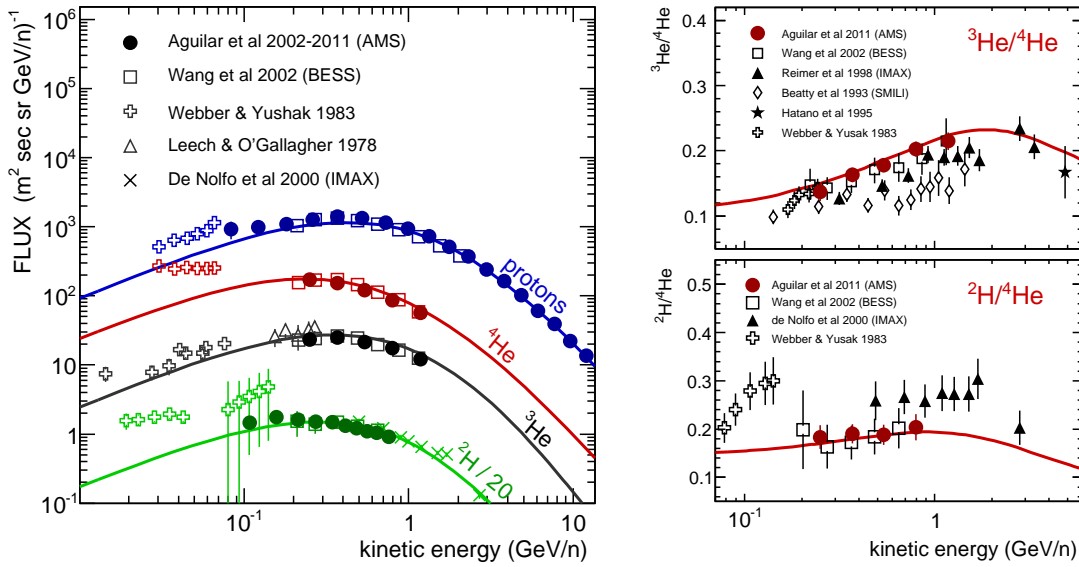


Fig. 1 Left: energy spectra of CR proton, deuteron (divided by 20), ^3He and ^4He . Right: isotopic ratios $^2\text{H}/^4\text{He}$ and $^3\text{He}/^4\text{He}$. Calculations are compared with the data from AMS-01 (Aguilar et al. 2002, 2011), IMAX (Reimer et al. 1998; De Nolfo et al. 2000), SMILI (Ahlen et al. 2000), BESS (Wang et al. 2002), Hatano et al. (1995), Leech & O’Gallagher (1978), Webber & Yushak (1983).

2 Observations

The AMS-01 experiment operated successfully in the STS-91 mission on board the space shuttle *Discovery*. The spectrometer was composed of a cylindrical permanent magnet, a silicon micro-strip tracker, time-of-flight scintillator planes, an aerogel Čerenkov counter and anti-coincidence counters. The performance of AMS-01 is described elsewhere (Aguilar et al. 2002). Data collection started on 1998 June 3 and lasted 10 days. AMS-01 observed cosmic rays at an altitude of ~ 380 km during a period, 1998 June, of relatively quiet solar activity. Results on isotopic spectra have been recently published in (Aguilar et al. 2011) with the ratios $^2\text{H}/^4\text{He}$, $^3\text{He}/^4\text{He}$, $^6\text{Li}/^7\text{Li}$, $^7\text{Be}/(^9\text{Be}+^{10}\text{Be})$ and $^{10}\text{B}/^{11}\text{B}$ in the range $\sim 0.2 - 1.5$ GeV of kinetic energy per nucleon. Fig. 1 shows the AMS-01 energy spectra of proton, deuteron, helium isotopes, and the ratios $^2\text{H}/^4\text{He}$ and $^3\text{He}/^4\text{He}$. The other data come from balloon borne experiments IMAX (Reimer et al. 1998; De Nolfo et al. 2000), SMILI (Ahlen et al. 2000), BESS (Wang et al. 2002), Hatano et al. (1995), Leech & O’Gallagher (1978) Webber & Yushak (1983).

The AMS-01 observations are made in a period, 1998 June, of relatively quiet solar activity, and the particle recorded are free from any atmospheric induced background. Furthermore, the AMS-01 material thickness between the top of the payload and the active detector amounted to $\sim 5 \text{ g cm}^{-2}$ which is considerably less than that of previous balloon borne experiments ($\sim 9\text{--}20 \text{ g cm}^{-2}$

of top-of-instrument material plus $\sim 5 \text{ g cm}^{-2}$ of residual atmosphere). Also important, for the aims of this work, is to realize that high precision data are currently flowing in from two active projects PAMELA and AMS-02, both operating in space. In particular, the data forthcoming by are expected to provide a dramatic improvement in our understanding of the CR transport processes and interactions (Tomassetti & Donato 2012; Coste et al. 2011; Oliva 2008).

3 CR Transport and Interactions

Galactic CR nuclei are believed to be accelerated by particle diffuse shock acceleration mechanisms occurring in galactic sites such as supernova remnants (SNRs). Their propagation in the ISM is dominated by particle transport in the turbulent magnetic field and interactions with the matter, that is generally described by a diffusion-transport equation including source distribution functions, magnetic diffusion, energy losses, hadronic interactions, decays, diffusive reacceleration and convective transport (the latter is not considered in this work). Models of CR propagation in the Galaxy employ fully analytical (Thoudam 2008; Tomassetti 2012), semi-analytical (Jones et al. 2001; Putze et al. 2010), or fully numerical calculation frameworks (Di Bernardo et al. 2010; Strong et al. 2007). The present work relies on the *diffusive-reacceleration* model implemented with GALPROP-v50.1p¹, which numeri-

¹<http://galprop.stanford.edu>

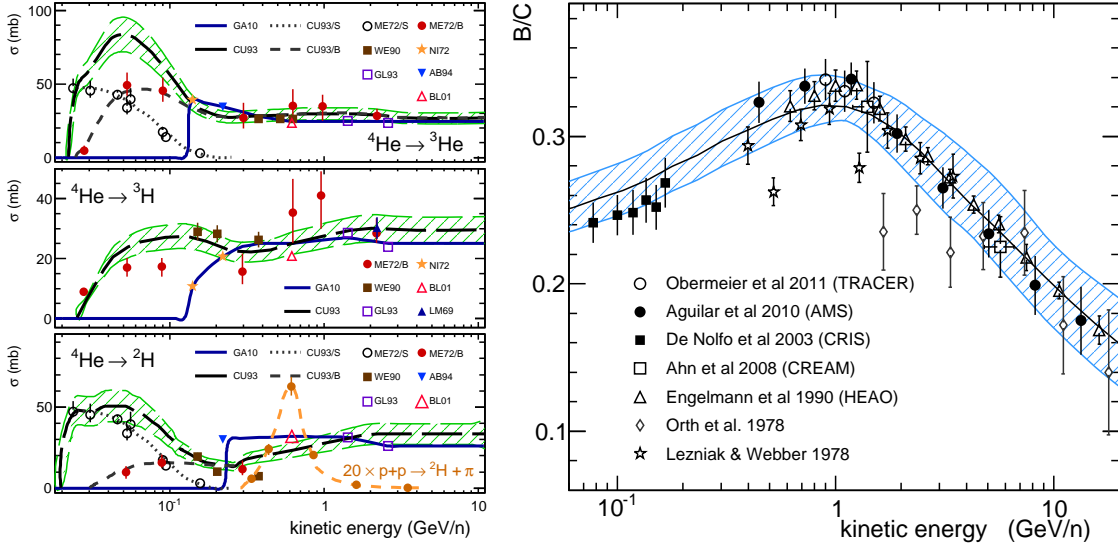


Fig. 2 Left: Cross section parametrizations (Cucinotta et al. 1993) for the channels ${}^4\text{He} \rightarrow {}^3\text{He}$, ${}^4\text{He} \rightarrow {}^3\text{H}$, ${}^4\text{He} \rightarrow {}^2\text{H}$ and $p+p \rightarrow \pi+{}^2\text{H}$ (multiplied by 20). The data are encoded as ME72: Meyer (1972), WE90: Webber (1990), NI72: Nicholls et al. (1972), GL93: Glagolev et al. (1993), AB94: Abdullin et al. (1994), BL01: Blinov et al. (2001), LM49: Lebowitz & Miller (1969), Right: B/C ratio from the CR propagation model of Table 1 and $1-\sigma$ uncertainty band. Data are from TRACER (Obermeier et al. 2011), AMS-01 (Aguilar et al. 2010), CRIS (De Nolfo et al. 2003), CREAM (Ahn et al. 2008), HEAO (Engelmann et al. 1990), Orth et al. (1978), and Lezniak & Webber (1978).

cally solves the cosmic ray propagation equation for a cylindrical diffusive region with a realistic interstellar gas distribution and source distribution.

3.1 Diffusive-Reacceleration Model

The propagation equation of the diffusive-reacceleration model for a CR species j is given by:

$$\begin{aligned} \frac{\partial \mathcal{N}_j}{\partial t} = & q_j^{\text{tot}} + \vec{\nabla} \cdot (D \vec{\nabla} \mathcal{N}_j) - \mathcal{N}_j \Gamma_j^{\text{tot}} \\ & + \frac{\partial}{\partial p} p^2 D_{pp} \frac{\partial}{\partial p} p^2 \mathcal{N}_j - \frac{\partial}{\partial p} (\dot{p}_j \mathcal{N}_j) \end{aligned} \quad (1)$$

where $\mathcal{N}_j = dN_j/dVdp$ is the CR density of the species i per unit of total momentum p .

The source term, $q_j^{\text{tot}} = q_j^{\text{pri}} + q_j^{\text{sec}}$, includes the primary acceleration spectrum (e.g. from SNRs) and the term arising from the secondary production in the ISM or decays. The primary spectrum is $q_j^{\text{pri}} = q_0 (R/R_B)^{-\nu}$, is normalized to the abundances, q_j^0 , at the reference rigidity R_B . The injection spectral indices are the same for all the primary elements. The source spatial distribution in the galactic disc is extracted from SNR observations. The secondary production term, $q_j^{\text{sec}} = \sum_k \mathcal{N}_k \Gamma_{k \rightarrow j}$, describe the products of decay and spallation of heavier CR progenitors with numer density \mathcal{N}_k . For collisions with the interstellar gas:

$$\Gamma_{k \rightarrow j} = \beta_k c \sum_{\text{ism}} \int_0^\infty n_{\text{ism}} \sigma_{k \rightarrow j}^{\text{ism}}(E, E') dE', \quad (2)$$

where n_{ism} are the number densities of the ISM nuclei, $n_H \approx 0.9 \text{ cm}^{-3}$ and $n_{He} \approx 0.1 \text{ cm}^{-3}$, and $\sigma_{k \rightarrow j}^{\text{ism}}$ are the fragmentation cross sections for the production of a j -type species at energy E from a k -type progenitor of energy E' in H or He targets. $\Gamma_j^{\text{tot}} = \beta_j c (n_H \sigma_{j,H}^{\text{tot}} + n_{He} \sigma_{j,He}^{\text{tot}}) + \frac{1}{\gamma_j \tau_j}$ is the total destruction rate for inelastic collisions (cross section σ^{tot}) and/or decay for unstable particles (lifetime τ). The spatial diffusion coefficient $D = D(\mathbf{r}, p)$ is taken as spatially homogeneous and rigidity dependent as $D(R) = \beta D_0 (R/R_0)^\delta$, where $R = pc/Ze$ is the rigidity, D_0 fixes the normalization at the reference rigidity R_0 , and the parameter δ specifies its rigidity dependence. Diffusive reacceleration is described as diffusion process acting in momentum space. It is determined by the coefficient D_{pp} for the momentum space diffusion:

$$D_{pp} = \frac{4p^2 v_A}{3\delta(4-\delta^2)(4-\delta)D} \quad (3)$$

where v_A is the Alfvén speed of plasma waves moving through the ISM. The last term describes Coulomb and ionization losses by means of the momentum loss rate \dot{p}_j .

GALPROP solves the steady-stady equation $\partial \mathcal{N}_j / \partial t = 0$ for a cylindrical diffusion region of radius r_{max} and half-thickness L with boundary conditions $\mathcal{N}_j(r=r_{\text{max}}) = 0$ and $\mathcal{N}_j(z=\pm L) = 0$. The local interstellar spectrum (LIS) is then computed for each species at the solar system coordinates $r_\odot = 8.5 \text{ kpc}$ and $z = 0$:

$$\Phi_j^{\text{LIS}}(E) = \frac{cA}{4\pi} \mathcal{N}_j(r_\odot, p), \quad (4)$$

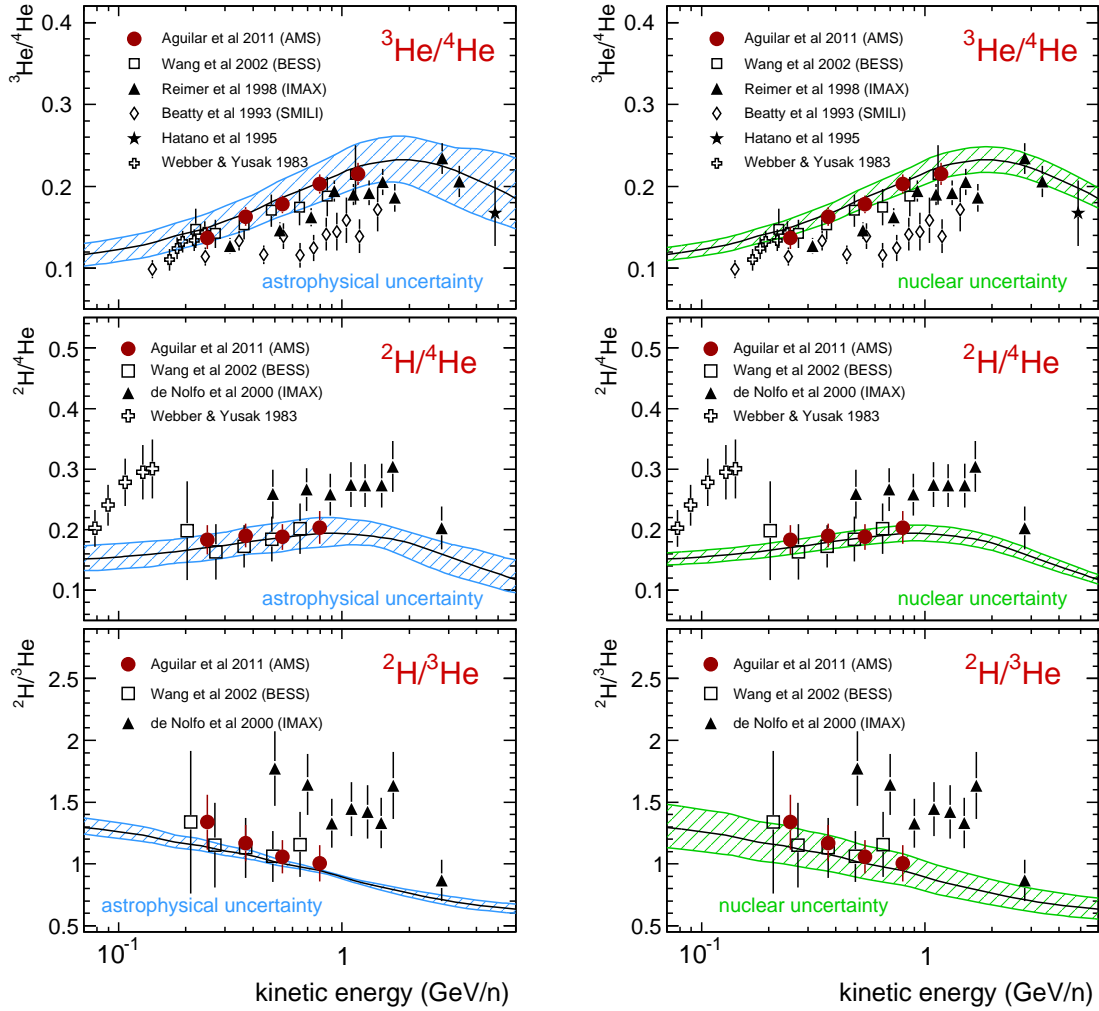


Fig. 3 Astrophysical (left) and nuclear (right) uncertainty bands for the predicted ratios ${}^2\text{H}/{}^4\text{He}$, ${}^3\text{He}/{}^4\text{He}$ and ${}^2\text{H}/{}^3\text{He}$ in comparison with the AMS-01 data. Other data are from IMAX (Reimer et al. 1998; De Nolfo et al. 2000), SMILI (Ahlen et al. 2000), BESS (Wang et al. 2002) Hatano et al. (1995), and Webber & Yushak (1983).

Table 1 Propagation parameter set.

Parameter	Name	Value
Injection, break value	R_B [GV]	9
Injection, index below R_B	ν_1	1.82
Injection, index above R_B	ν_2	2.36
Diffusion, magnitude	D_0 [$\text{cm}^2 \text{s}^{-1}$]	$5.75 \cdot 10^{28}$
Diffusion, index	δ	0.34
Diffusion, ref. rigidity	R_0 [GV]	4
Reacceleration, Alfvén speed	v_A [km s^{-1}]	36
Galactic halo, radius	\mathcal{R} [kpc]	20
Galactic halo, height	z_h [kpc]	4
Solar modulation parameter	ϕ [MV]	500

where A is the mass number and the flux Φ^{LIS} is given in units of kinetic energy per nucleon E . For the description we adopt the “conventional model” which finely reproduces the CR elemental fluxes at intermediate energies of $\sim 100 \text{ MeV} - 100 \text{ GeV}$ per nucleon.

3.2 Heliospheric Propagation

CRs in the solar neighbourhood undergo convection, diffusion and energy changes as results of the expansion of the solar wind. To describe the solar modulation effect, we adopt the so-called *force-field approximation* that arise from the a spherically symmetric description of the heliosphere (Gleeson & Axford 1968). The correspondence between the (modulated) top-of-atmosphere spectrum, Φ^{TOA} , and the (unmodulated) LIS spectrum of 4, Φ^{LIS} , is expressed

by the effective parameter ϕ (GV) through:

$$\Phi^{\text{IS}}(E^{\text{IS}}) = \left(\frac{p^{\text{IS}}}{p}\right)^2 \Phi^{\text{TOA}}(E^{\text{TOA}}), \quad (5)$$

where the LIS and TOA energies per nucleon are related by $E^{\text{IS}} = E^{\text{TOA}} + \frac{Z}{A}\phi$. The main parameters of the model are listed in Table 1. The remaining specifications are as in the file `galdef_50p_599278` provided with the package.

3.3 Fragmentation Cross Sections

To compute the secondary nuclei production rate from the disintegration of the heavier CR nuclei, a large amount of cross section estimates is required. The accuracy of the calculated secondary spectra therefore depends on the reliability of the production and destruction cross sections employed.

The production of ^2H and ^3He isotopes is mainly due to collision of ^4He nuclei. The ^3He isotopes are also produced via decay of tritium ($^3\text{H} \rightarrow ^3\text{He}$) which, in turn, is predominantly created by ^4He spallation. The most relevant *projectile* \rightarrow *fragment* processes for the ^3He abundance are $^4\text{He} \rightarrow ^3\text{He}$ and $^4\text{He} \rightarrow ^3\text{H}$. The main deuteron production channel is $^4\text{He} \rightarrow ^2\text{H}$. Low energy deuterons are also created by the fusion reaction $p + p \rightarrow \pi + ^2\text{H}$ acting between ~ 300 and ~ 900 MeV of the proton energy (Meyer 1972). Although the p - p fusion cross section is very small ($\sigma \sim 3$ mb), this reaction contributes appreciably to the ^2H abundance because of the large CR proton flux. Spallation of heavier nuclei (C, O, Fe) give a minor contribution, roughly $\lesssim 10\%$ of their fractional abundance. For all these channels the total inclusive reaction can be realized in a number of possible final states. We employ the phenomenological parametrization of Cucinotta et al. (1993). These parametrizations are shown in Fig. 2 together with the accelerator data. For ^2H and ^3He , the partial contributions of break-up (B) and stripping (S) reactions are shown separately.

For all these processes we have assumed that the fragment is ejected with the same the kinetic energy per nucleon E of the projectile, E' . This *straight-ahead* approximation, expressed by $\sigma(E, E') \approx \sigma(E)\delta(E - E')$, has been validated within some percent of accuracy for reactions involving $Z > 2$ nuclei (Kneller et al. 2003) and for lighter species ($Z < 3$) (Cucinotta et al. 1993). For the p - p fusion channel, the kinetic energy per nucleon is not conserved due to the kinematic of the reaction: the energy of ejected deuterons is systematically lower than that of the proton of a factor ~ 4 on average. Using a *straight-ahead* fashion, we write $\sigma(E, E') \approx \sigma(E)\delta(E - \xi E')$, where $\xi \cong 4$ is the average inelasticity of the ^2H . The p - p fusion contributes to the ^2H flux at energies below ~ 250 MeV nucleon $^{-1}$. For nuclear reactions involving heavier ($Z > 2$) nuclei, we use the

default cross section parametrization of GALPROP. To account for CR collisions with the interstellar helium ($\sim 10\%$ of the ISM) the parametrization of Ferrando et al. (1988) is used. Calculation of CR spectra and ratios $^2\text{H}/^4\text{He}$ and $^3\text{He}/^4\text{He}$ are shown in Fig. 1 for the modulation intensity of $\phi = 500$ MV.

4 Model Uncertainties

We consider two classes of uncertainty in the model estimates. The *astrophysical uncertainties* are those associated with the transport parameters constrained by the B/C ratio. The relevant parameters for the secondary productions are δ , v_A and the ratio D_0/L . We perform a grid scan in the parameter space $\{\delta, v_A, D_0/L\}$ by running GALPROP multiple times. The other parameters, *e.g.* the source parameters and the modulation potential, are kept fixed. For each parameter configuration, we select the B/C-compatible models within one sigma of uncertainty in the χ^2 statistics. We use B/C data from HEAO (Engelmann et al. 1990), CREAM (Ahn et al. 2008), AMS-01 (Aguilar et al. 2010) and Orth et al. (1978). Fig. 2 illustrates the uncertainty band derived by this procedure. Note that this method has severe limitations and allows to simultaneously explore only some parameters. More robust strategies require advanced statistical tools, see *e.g.* Trotta et al. (2011), Putze et al. (2010) and in particular Coste et al. (2011). However the purpose in this work is estimating the parameter uncertainties rather than determining their exact values.

The *nuclear uncertainties* on the ^2H and ^3He calculations are those arising from uncertainties in their production cross sections. In order to estimate the cross section uncertainties using the information from the measurements, we re-fit the parametrizations with the data to determine their overall normalizations and associated errors. The uncertainty bands are shown in Fig. 2 for the main reactions of ^2H and ^3He production. These uncertainties can be directly translated into error bands for the predicted ratios $^2\text{H}/^4\text{He}$ and $^3\text{He}/^4\text{He}$. These uncertainty bands are shown in Fig. 3.

The AMS-01 data agree well with calculations within the astrophysical band, indicating consistency with the propagation picture arising from the B/C analysis. It is also clear that $Z \leq 2$ nuclear ratios carry valuable information on the transport parameters, *i.e.*, they can be in principle used to tighten the constraints given by the B/C ratio. On the other hand, the *nuclear uncertainties* represent an intrinsic limitation on the accuracy of the model predictions, as reported in the right panels of the figure. Only precise cross section data or more refined calculations may pin down these uncertainties. Unaccounted errors or systematic biases in cross section estimates cause errors on the predicted ratios which, in turn, may lead to a mis-determination of the CR

transport parameters. Given the level of precision expected from PAMELA or AMS-02, systematic errors in the cross section data may represent the dominant source of uncertainty for the model predictions of light CR isotopes. A strategy to check the model consistency with CR data is the use of secondary to secondary ratios such as ${}^2\text{H}/{}^3\text{He}$. In fact, the ${}^2\text{H}$ and ${}^3\text{He}$ isotopes have the same astrophysical origin and similar progenitors (mainly ${}^4\text{He}$). Thus, their ratio is almost insensitive to the propagation physics and can be used to probe the net effect of the nuclear interactions. In fact, a mis-consistency between calculations and ${}^2\text{H}/{}^3\text{He}$ data would indicate the presence of systematic biases in the cross sections that cannot be re-absorbed by the propagation parameters. As illustrated in the bottom panels of Fig. 3, the tight astrophysical uncertainty band (left) indicates a little discrepancy between data and model which can be understood if one consider the nuclear uncertainty (right), which is dominant for the ${}^2\text{H}/{}^3\text{He}$ ratio. Similarly, the use of other ratios such as ${}^6\text{Li}/{}^7\text{Li}$, Li/Be or ${}^{10}\text{B}/{}^{11}\text{B}$ can represent a useful diagnostic tool for testing the overall consistency of the model.

5 Conclusions

We have compared new observations of the ${}^2\text{H}/{}^4\text{He}$ and ${}^3\text{He}/{}^4\text{He}$ ratios in CRs made by the AMS-01 experiments with standard calculations of secondary production in the ISM. These ratios are well described by propagation models consistent with B/C ratio under a *diffusive-reacceleration* scenario, suggesting the He and heavier nuclei such as C-N-O experience similar propagation histories. The accuracy of the secondary CR calculations relies on the accuracy of the cross sections employed. Given the level of precision expected from AMS-02, the errors in the cross section data will likely represent the dominant source of uncertainty for the model predictions of rare CR isotopes such as ${}^2\text{H}$ or ${}^3\text{He}$. Similar issues may concern for ${}^6,7\text{Li}$, ${}^{7,9,10}\text{Be}$, or ${}^{10,11}\text{B}$. These errors may be reduced using more refined calculations or more precise accelerator data. For example, future observations may require the departure from the straight-ahead approximation which is generally assumed in the CR propagation studies for light nuclei. Possible consistency checks for propagation models can be done using the secondary to secondary ratios, which are less sensitive to the astrophysical aspects of the interstellar CR propagation. The use of ratios such as ${}^2\text{H}/{}^3\text{He}$, ${}^6\text{Li}/{}^7\text{Li}$ or ${}^{10}\text{B}/{}^{11}\text{B}$ can represent a useful diagnostic test for the reliability of the calculations: any CR propagation model, once tuned on secondary to primary ratios, must correctly reproduce the secondary to secondary ratios as well. Another model limitation concerns the solar modulation effect. Any more refined modeling requires to leave the force field approximation, that may be

too simple to finely reproduce the future data of different A/Z isotopes. Our understanding of the CR heliospheric propagation may be dramatically improved by the AMS-02 long-term observations of different CR species.

6 Acknowledgments

I thank my many colleagues in AMS for helpful discussions and F. Focacci for her bibliographic support. This work is supported by *Agenzia Spaziale Italiana* under contract ASI-INFN 075/09/0.

References

- Abdullin, S. K., et al., 1994, *Nuc. Phys. A*, 569, 753 (AB94)
 Aguilar, M., et al.2011, *ApJ*, 746, 105 (AMS-01)
 Aguilar, M., et al.2010, *ApJ*, 724, 329–340 (AMS-01)
 Aguilar, M., et al.2002, *Phys. Rept.*, 366, 331–405 (AMS-01)
 Ahlen, S. P., et al.2000, *ApJ*, 534, 757–769 (SMILI-II)
 Ahn, H. S., et al.2008, *Aph*, 30–3, 133–141. (CREAM)
 Blinov, A. V., Chadeyeva, M. V., Grechko V. E., & Turov V. F. 2001, *Phys. Atom. Nucl.*, 64, 907 (BL01)
 Coste, B, Derome, L., Maurin, D., & Putze, A., 2012, *A&A*, 539, 88
 Cucinotta, M. G., Townsend, L. W., & Tripathi, R. K., NASA–TR 3285, 1993
 De Nolfo, G. A., et al.2003, *Proc 28th (Tsukuba)*, 2, 1667–1670. (CRIS)
 De Nolfo G.A. et al., 2000, in *Proc. ACE2000 Symp.*, ed. Mewaldt R.A. et al.(AIP: NY), AIP 528, 425 (IMAX)
 Di Bernardo, G., Evoli, C., Gaggero, D., Grasso, D., & Maccione, L., 2010, *Aph*, 34–5, 274–283
 Donato, F., Fornengo, N., & Maurin, D., 2008, *PRD*, 78, 043506
 Engelmann, J. J., et al., 1990, *ApJ*, 233, 96–111. (HEAO3-C2)
 Evoli, C., Cholis, I., Grasso, D, Maccione, L., & Ullio, P., arXiv: astro-ph/1108.0664
 Ferrando, P., et al., 1988, *PRC*, 37–4, 1490–1502
 Glagolev, V. V., et al., 1993, *Z. Phys. C*, 60, 421 (GL93)
 Gleeson, L. J., & Axford, W. I 1968, *ApJ*, 154, 1011
 Hatano, Y., Fukada, Y., Saito, Y., Oda, H., & Yanagita, T. 1995, *PRD*, 52, 6219–6223
 Jones, F. C., Lukasiak, A, Ptuskin, V., & Webber, W., 2001, *ApJ*, 547, 264.
 Kneller, J. P., Phillips, J. R., & Walker, T. P., 2003, *ApJ*, 589, 217–224
 Lebowitz, E., & Miller, J. M., 1969, *Phys. Rev.*, 177, 1548 (LM69)
 Leech, H. W., & O’Gallagher, J. J. 1978, *ApJ*, 221, 1110
 Lezniak, J. A., & Webber, W. R., 1978, *ApJ*, 223, 676–696.
 Meyer, J. P., 1972, *A&A Suppl.*, 7, 417–467
 Nicholls, J. E., et al., 1972, *Nuc. Phys. A*, 181, 329 (NI72)
 Obermeier, A., Ave, M., Boyle, P. J., Höppner, C., Hörandel, J., R., & Müller, D., 2011, *ApJ*, 742, 14 (TRACER)
 Oliva, A., 2008, *NIM A*, 588, 255–258 (AMS-02)
 Orth, C. D., et al., 1978, *ApJ*, 226, 1147–1161
 Putze, A., Derome, L., & Maurin, D., 2010, *A&A*, 516, 66
 Reimer, O., et al.1998, *ApJ*, 496, 490 (IMAX)
 Salati, P., Donato, F. & Fornengo, N., arXiv: astro-ph/1003.4124

-
- Strong, A. W., Moskalenko, I. V., & Ptuskin, V. S., 2007, *Ann. Rev. of Nucl. & Part. Sci.*, 57, 285–327
- Thoudam, S., 2008, *MNRAS*, 388, 335–346
- Tomassetti, N., 2012, *ApJ*, 752, L13
- Tomassetti, N., & Donato, F., 2012, *A&A*, 544, A16
- Trotta, R., et al., 2011, *ApJ*, 729, 106–122 (*GALPROP*)
- Wang, J. Z., et al., 2002, *ApJ*, 564, 244–259 (*BESS*)
- Webber, W. R., 1997, *Ad.Sp.Res.*, 19–5, 755–758
- Webber, W. R., 1990, in *AIP Conf. Proc.* 203, ed. W. V. Jones et al.
- Webber, W. R., & Yushak, S. M., 1983, *ApJ*, 275, 391–404